Computer Physics Communications 129 (2000) 256–266

Computer Physics Communications

www.elsevier.nl/locate/cpc

Lattice dependence of reaction-diffusion in lattice Boltzmann modeling

Ronald Blaak [1], Peter M.A. Sloot *

University of Amsterdam, Faculty for Mathematics, Computer Science Physics and Astronomy, Section Computational Science, Kruislaan 403, 1098 SJ Amsterdam, The Netherlands

Abstract

We consider the influence of the lattice symmetry and size of the lattice Boltzmann method on the behavior of a pure reaction diffusion system. We show that the effect of the dispersion relation in the diffusion coefficient can be minimized, by tuning the fraction of rest particles and the relaxation parameter. For the reaction, we focus on the Selkov model and study the dynamics of pattern formation due to the Turing Instability. For the chosen reaction parameters, however, no clear influence of the lattice symmetry is found.

PACS: 47.11.+j; 47.54.+r

Keywords: Lattice-Boltzmann method; Reaction-diffusion; Lattice symmetry; Pattern formation

1. Introduction

In the last few years a lot of attention is paid to reaction diffusion systems. Experimental and numerical results have shown that these in principle simple systems show a wide variety of complex behaviors, such as chemical waves, oscillations and non-homogeneous patterns [1–3]. These systems are for instance formed by a number of chemical species which are dissolved in some fluid and are able to chemically interact with each other forming new compounds. The macroscopic equations which govern these phenomena, as well as the general behavior of these systems, can also be observed in different models and or simulations, e.g., population dynamics.

The chemical species are allowed to react, which gives rise to a dynamical process to form a steady state or dynamically stable cycle. By tuning the reaction parameters, one is able to change this process such that the final outcome is a homogeneous state, a stable pattern, formed by domains where different chemically species are dominant, or an oscillating state.

In general such a reaction-diffusion system can be described by the following set of coupled equations:

$$\frac{\partial \rho_s}{\partial t} - D_s \nabla^2 \rho_s = R_s, \tag{1}$$

where t is the time, ∇^2 the Laplacian operator with respect to the spatial coordinate x, $\rho_s(x,t)$ the mass density and D_s is the diffusion coefficient. The subscript s is a label for the different chemical species.

* Corresponding author. E-mail: sloot@wins.uva.nl.

[1] E-mail: ronaldb@wins.uva.nl.

0010-4655/00/$ – see front matter
PII: S0010-4655(00)00112-0

The right-hand side of the equation, R_s, represents the reaction term and will in general depend on the local densities of all chemical species and the reaction mechanism governing this system. In reality the reaction term should also depend on the temperature, specially since reaction will produce energy which will locally heat up the system. However, we will assume our model to be a-thermal.

In order to model more realistic systems large system sizes are required. For that reason we adopt the lattice Boltzmann formalism to simulate such systems [4], because this method is ideally suited for parallel execution, thus supporting large system sizes [5]. Moreover it is also able to deal with complicated geometries [6] and changing environments, e.g., aggregation processes [7].

In this article we will investigate how the system size and the symmetry of the underlying lattice will influence the behavior of the system. If one is interested in the steady state solution of a reaction-diffusion system only, this is in principle not necessary. Provided the system size which is modeled is large enough, it is conceivable that the lattice symmetry is not too important any steady state could be obtained.

If one is interested in dynamical modeling of problems like ground water contamination and bioremediation, however, the lattice symmetry might be important. The reason is that at a local level and short time scales the lattice symmetry might influence the dynamical behavior of reaction diffusion processes. In order to investigate this influence, we have performed a series of simulations on the formation of Turing patterns [8] in the Selkov model [9]. The choice for this particular model is based on its simplicity and the fact that much is known about it.

The remaining of this article is organized as follows. In Section 2 we explain the model we used to simulate the reaction diffusion. In Section 3 we compare the predicted diffusion coefficient with the one from simulations. In Section 4 the Selkov model is discussed in some more detail. In Section 5 we present our results on the size and symmetry dependence of the simulations. In Section 6 we consider the influence of the boundaries. In Section 7 we finish with a discussion of our results and suggestions for future research.

2. Model

In order to model the reaction-diffusion equations (1), we will use the lattice-Boltzmann scheme. The one-particle distribution of species s at time t, position $\vec{x}$ and with velocity $\vec{e}_i$ is denoted by $f_s(\vec{x}, i, t)$. In case of a hexagonal lattice the nearest neighbor vectors are given by

$$\vec{e}_i = \begin{cases} (0,0), & i = 0, \\ (\cos(\theta_i), \sin(\theta_i)), & \theta_i = (i-1)\pi/3, \\ & 1 \leqslant i \leqslant 6, \end{cases} \tag{2}$$

and in the case of a square lattice by

$$\vec{e}_i = \begin{cases} (0,0), & i = 0, \\ (\cos(\theta_i), \sin(\theta_i)), & \theta_i = (i-1)\pi/2, \\ & 1 \leqslant i \leqslant 4, \\ \sqrt{2}(\cos(\theta_i), \sin(\theta_i)), & \theta_i = (i-5)\pi/2 + \pi/4, \\ & 5 \leqslant i \leqslant 8. \end{cases} \tag{3}$$

The lattice Boltzmann equation for $f_s(\vec{x}, i, t)$ can be written as

$$f_s(\vec{x} + \vec{e}_i, i, t+1) - f_s(\vec{x}, i, t) = \Omega_s(\vec{x}, i, t), \tag{4}$$

where $\Omega_s(\vec{x}, i, t)$ is the collision operator of species s. This term consists of a reactive term Ω_s^{R} and non-reactive term Ω_s^{NR}. For the non-reactive part of the collision we use the normal single relaxation time BGK approximation:

$$\Omega_s^{\mathrm{NR}}(\vec{x}, i, t) = -\frac{1}{\tau_s}\big(f_s(\vec{x}, i, t) - f_s^{\mathrm{eq}}(\vec{x}, i, t)\big), \tag{5}$$

where the equilibrium density f_s^{eq} depends on the local density ρ_s and local velocity $\vec{u}$. In the normal lattice Boltzmann simulation this equilibrium distribution for is given by

$$f_s^{\mathrm{eq}}(\vec{x}, i, t) = w_{s,i}\rho_s\left(1 + \frac{(\vec{e}_i \cdot \vec{u})}{c_s^2} + \frac{(\vec{e}_i \cdot \vec{u})^2}{2c_s^4} - \frac{\vec{u}^2}{2c_s^2}\right), \tag{6}$$

where c_s in the speed of sound. The weights $w_{s,i}$ are dependent on the lattice symmetry, and result in

$$w_{s,i} = \begin{cases} z_s, & i = 0, \\ (1 - z_s)/6, & 1 \leqslant i \leqslant 6 \end{cases} \tag{7}$$

for a hexagonal lattice, where z_s denotes the fraction of rest particles and can be different for different species. For a square lattice we find

$$w_{s,i} = \begin{cases} z_s, & i = 0, \\ (1-z_s)/5, & 1 \leqslant i \leqslant 4, \\ (1-z_s)/20, & 5 \leqslant i \leqslant 8. \end{cases} \tag{8}$$

Since we are modeling a system where the chemical species are dissolved in a fluid, the velocity $\vec{u}$, can be replaced by the local velocity of the solvent, which for low concentrations will hardly be influenced by the reactants. In what follows, however, we will consider a pure reaction diffusion system, and hence the average mean flow will be zero, this leads to the reduction of the equilibrium distribution function to

$$f_s^{\mathrm{eq}}(\vec{x}, i, t) = w_{s,i}\rho_s = w_{s,i}\sum_i f_s(\vec{x}, i, t). \tag{9}$$

For the reactive part of the collision term, we will follow Dawson et al. [4], and assume that R_s the change in density of species s due to a reaction, will be distributed over the different directions, proportional to the weights of pure diffusion

$$\Omega_s^{\mathrm{R}} = w_{s,i}R_s. \tag{10}$$

The exact form the reaction term R_s, still needs to be specified. It depends on the set of reactions one is interested in, and can be very complicated. In our application we will assume that it only depends on the local densities of the reacting species, however it should be noted that in reality this might also depend on the velocity dependent cross-sections for the reaction.

If we assume $f \approx f^{\mathrm{eq}} + \epsilon f^{(1)}$, $\partial/\partial t \propto \epsilon^2$, $\partial/\partial\vec{x} \propto \epsilon$, and $R_s \propto \epsilon^2$, where ϵ is a small parameter, a Taylor series of $f_s(\vec{x} + \vec{e}_i, i, t)$ around $f_s(\vec{x}, i, t)$ will lead to the desired evolution equation (1) for ρ_s [4], and the diffusion coefficient D_s results in

$$D_s = \tfrac{1}{2}(1-z_s)\big(\tau_s - \tfrac{1}{2}\big) \quad \text{hexagonal lattice,} \tag{11}$$

$$D_s = \tfrac{3}{5}(1-z_s)\big(\tau_s - \tfrac{1}{2}\big) \quad \text{square lattice.} \tag{12}$$

In the case of pure diffusion, as we intend to use initially, this fraction can be chosen arbitrary to meet external constraints. If one is interested in the application including flow, these values are chosen to be $z_s = 1/2$ for the hexagonal and $z_s = 4/9$ for the square lattice, in order to retrieve the Navier–Stokes equations. Note that the relaxation parameter has to be chosen larger than a half, otherwise unphysical behavior is obtained.

3. Diffusion coefficient

In order to measure the diffusion coefficient we use a non-reactive system in which we impose initially a concentration wave of a sinusoidal shape $\rho(\vec{x}, t = 0) = 1 + \epsilon\cos(\vec{k}\cdot\vec{x})$ for some wave vector $\vec{k}$. This wave vector should however be chosen such that it fits on the lattice, e.g., $\vec{k} = (2\pi i/N_x\hat{x}, 2\pi j/N_y\hat{y})$.

If this density profile is applied to the diffusion equation we find that it has an exponential decay given by

$$\rho(\vec{x}, t) = \rho(\vec{x}, 0)\mathrm{e}^{-Dk^2t}. \tag{13}$$

In Fig. 1 we have plotted the measured diffusion coefficient and its relative error as a function of the relaxation parameter for several wave vectors. In order to measure the diffusion, the decay of the imposed amplitude as function of the time is fitted to an exponential. Although the simulations are performed on a 256×256 grid, this is not strictly necessary for all wave vectors. The only requirement for a given wave vector is that it should fit an integer number of times on the lattice, hence, depending on the wave vector, smaller lattices can be used. The wave vectors shown here are $\vec{k} = (i2\pi/256, j2\pi/256)$ with $i, j = 0, 1, 2, 4, 8$.

It can be seen that the behavior of the measured diffusion coefficients for different wave vectors is self-similar an can, for larger relaxation parameters, be mapped on each other. However, it is clear that for $\tau > 5$ the deviations from the predicted diffusion coefficient become too large for out purposes. The relative error of indicates that also for small relaxation parameters the measured and predicted value disagree increasingly for larger wave vectors. In first approximation, however, the curves share a common value for the relaxation parameter is optimal.

The origin of the deviation of the measured diffusion from the predicted one, lies in the decay of the amplitude of the imposed density profile. For small values of $\tau \gtrsim 0.5$ the relaxation goes fast, which lead to numerical instabilities in simulations causing initial oscillations, rather than a perfect exponential decay.

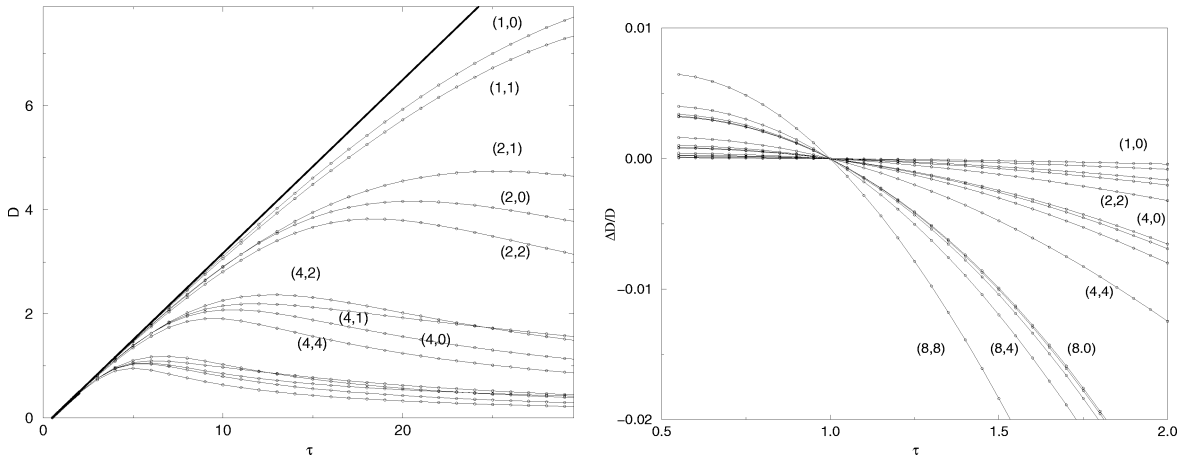

(a) (b)

Fig. 1. (a) The measured diffusion coefficient D as function of the relaxation parameter τ. The straight line is the theoretical value. (b) The relative error in the measured diffusion coefficient as a function of the relaxation parameter for small τ. The measurements are done on a 256×256 square lattice with the fraction of rest particles z is fixed to $4/9$. The labeling of a curve (i, j) correspond to the wave vector $\frac{2\pi}{256}(i, j)$.

The diffusion coefficient, however, will be given reasonable accurate. For large τ the measured and predicted value of the diffusion start to disagree. Due to the numerical scheme, the amplitude is not decaying exponentially all the time, but can grow for small periods.

The discrepancy between the measured and predicted value of the diffusion coefficient, will put some constraints on the simulation parameters used. Depending on the range of interest, there are a few simple solutions, of which the simplest would be taking a bigger lattice size. To avoid both described effects in the decay, one should take the relaxation parameter of the order unity. In order to access larger diffusion coefficients, one could use multiple time steps.

For pure reaction diffusion however, there is also another option. Since the equilibrium distribution does not depend on the local velocity, one can chose different weights, allowing to set a different value for the diffusion. This can only be done, because they were fixed by the requirement to retrieve the Navier–Stokes equations. In Fig. 2 the relative error of the diffusion is plotted as a function of the fraction of fixed particles, for $\tau = 1$ and several wave vectors. Also here the discrepancy increases for larger wave vectors.

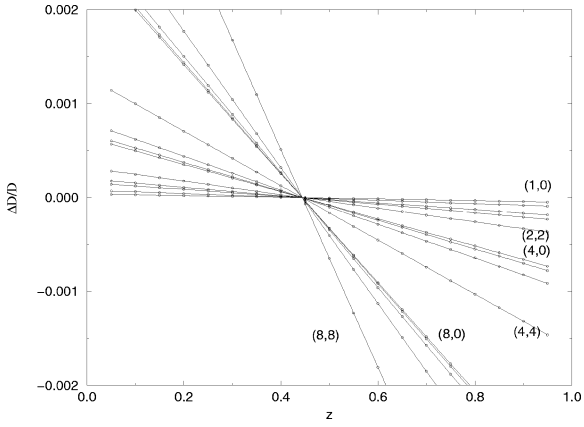

Fig. 2. The relative error in the measured diffusion coefficient as a function of the fraction of rest particles z. Different curves correspond to different wave vectors in magnitude and direction on a 256×256 square lattice, with the relaxation parameter $\tau = 1$. The labeling of a curve (i, j) correspond to the wave vector $\frac{2\pi}{256}(i, j)$.

For different values of the fraction of rest particles z, figures similar to Fig. 1 are obtained. However, this leads to a shift of the "optimal" value for the relaxation parameter. In case of the square grid for $z = 3/9$, $4/9$ and $5/9$ this value is given by respectively $\tau \approx 1.07$, 1.00 and 0.96. Since smaller z and larger τ

both increase the diffusion coefficient (11), this can be used to simulate a diffusion coefficient which is less sensitive to a dispersion relation.

Although the theoretical diffusion coefficient, which is obtained from the Chapmann–Enskog expansion, is independent of the wave vector, this is obviously not true. In order to eliminate this effect as much as possible the values of the relaxation parameter and the fraction of rest particles should be chosen appropriately. For the fraction of rest particles, we keep the values as used for normal LBM simulations. The main reason for this choice is that in future applications the incorporation of low flow fields is needed and we don not pursue the direction of pure reaction-diffusion, where this value could possibly be optimized. The same is true for the relaxation parameter, which normally would be close to unity. However in order the obtain a sufficient range of diffusion constants, we allow it to be chosen in the range $(0.55, 2.0)$.

The existence of the dispersion relation, however, will in general affect the simulations. The deviation of the diffusion coefficient from the predicted one, will show up mainly in the larger wave vectors and hence smaller length scales. Depending on the application this will influence the outcome of the simulation. In our case, where we will focus on the formation of patterns, this could for instance influence the shape of the spots that appear in the pattern. The relevant length scale of the pattern is an order of magnitude larger and will be influenced less.

4. Selkov

The Selkov model consists of a system of three coupled chemical reactions, involving four species [9]

$$A \underset{k_{-1}}{\overset{k_1}{\rightleftharpoons}} X, \tag{14a}$$

$$X + 2Y \underset{k_{-2}}{\overset{k_2}{\rightleftharpoons}} 3Y, \tag{14b}$$

$$Y \underset{k_{-3}}{\overset{k_3}{\rightleftharpoons}} B. \tag{14c}$$

It is assumed that the densities of A and B are fixed by external sources. This results in only two evolution equations, determined by the densities and the reaction rates k_i

$$\frac{\partial \rho_X}{\partial t} - D_X \nabla^2 \rho_X = R_X = k_1 \rho_A - k_{-1}\rho_X - k_2 \rho_X \rho_Y^2 + k_{-2}\rho_Y^3, \tag{15a}$$

$$\frac{\partial \rho_Y}{\partial t} - D_Y \nabla^2 \rho_Y = R_Y = k_{-3}\rho_B - k_3 \rho_Y + k_2 \rho_X \rho_Y^2 - k_{-2}\rho_Y^3. \tag{15b}$$

By solving the equations $R_X = R_Y = 0$, we find that there are at most three fixed points. In order to determine the linear stability of the fixed point with density ρ_X^* and ρ_Y^*, we study the exponential decay of a homogeneous distortion $\vec{\rho}^* + \vec{\epsilon}\exp(\lambda t)$. This gives a simple eigenvalue problem $\partial_t \vec{\rho} = L\vec{\rho}$, where $L_{ij} = \partial R_i/\partial \rho_j$ and results in the eigenvalue equation

$$\lambda^2 - \mathrm{Tr}(L)\lambda + |L| = 0. \tag{16}$$

For a stable solution we require $\mathrm{Re}(\lambda_\pm) < 0$. In the case of two complex solutions this means that $L_{11} + L_{22} < 0$, in the case of two real solutions there is an additional constraint, the determinant of the matrix L should be positive, otherwise there would exist both a negative and positive eigenvalue, hence, a stable and unstable mode. In the last case the simulation will go directly to the stable fixed point, while in the first case the density will spiral to that point.

If the ratio of the diffusion coefficients D_X/D_Y becomes larger than a critical value, the Selkov model develops a Turing instability. The fixed point becomes linearly unstable against perturbations of the form $\delta\vec{\rho} = \sum_{\vec{\xi}} \vec{A}_{\vec{\xi}} e^{\imath \vec{\xi}\cdot\vec{x}}$. For a complete analysis we refer to [10], while we give here only the main results. The critical ratio of the diffusion coefficients is given by

$$\frac{D_X}{D_Y} = \frac{L_{XX}L_{YY} - 2L_{XY}L_{YX}}{L_{YY}^2} + \frac{2\sqrt{L_{XY}L_{YX}(L_{XY}L_{YX} - L_{XX}L_{YY})}}{L_{YY}^2}. \tag{17}$$

If the ratio of the diffusion coefficients is larger than this critical ratio the Turing instability is guaranteed for those wave vectors ξ which satisfy $|\xi_-| \leqslant |\xi| \leqslant |\xi_+|$ where $|\xi^2|_\pm$ is given by

$$|\xi^2|_\pm = \frac{D_X L_{YY} + D_Y L_{XX}}{2D_X D_Y |L|} \pm \frac{\sqrt{(D_X L_{YY} + D_Y L_{XX})^2 - 4|L| D_X D_Y}}{2D_X D_Y |L|}. \tag{18}$$

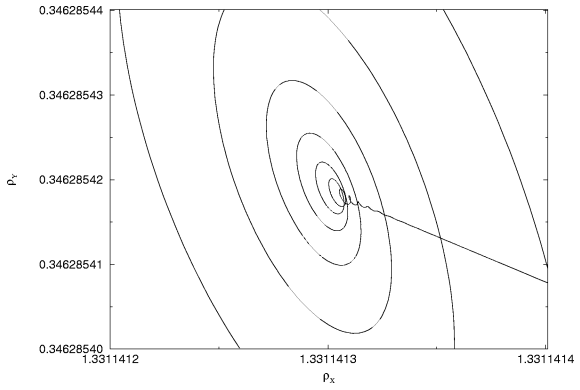

Fig. 3. Enlargement of the path followed by the average densities in time. This is the result of a simulation on a 256×256 square grid where the spiraling behavior is ended after approximately 20 thousand time steps.

5. Results

We have performed simulation of various lattice sizes. We prepare the initial densities of both simulated species in the Selkov model, by an average density, corresponding to the homogeneous solution of the reaction equations, with a random noise of about one percent. We have chosen he reaction parameters $k_1\rho_A = 2.65667 \times 10^{-3}$, $k_{-1} = 6.65 \times 10^{-4}$, $k_2 = k_{-2} = 1.5 \times 10^{-2}$, $k_{-3}\rho_B = 5.313334 \times 10^{-4}$ and $k_3 = 6.65 \times 10^{-3}$ [4]. The diffusion coefficients are set to $D_X = 0.2914$ and $D_Y = 0.017$, which ensures that the ratio $D_X/D_Y = 17.1412$ is above the critical value 16.2121. Under these conditions most of the patterns formed in simulations with sizes $32m \times 32n$ lead to the formation of spots in a hexagonal type arrangement. If the system size is to small, e.g., 32×32, homogeneous density distributions are found, and by narrowing only one of the lattice dimensions a pattern of stripes is formed. In principle other patterns, e.g., arrangements with square symmetry, could be obtained by, initializing the densities of both species with specific modulations, however, these are easily distorted.

In Fig. 3 an enlargement of the path of the average densities followed by both species in time, is shown for a system on a square lattice with size 256×256. It follows an inward spiral towards the stable fixed point of the reaction equations, as can be expected on the basis of the stability analysis. However, when the fixed point is approached after approximately 20 thousand time steps, the solution starts to run away from this initial goal. What has happened is that the reaction equations initially hold not only locally but also on average for the whole system, leading to the spiral path. In the neighborhood of the fixed point however, the stable fluctuations are probed, forming

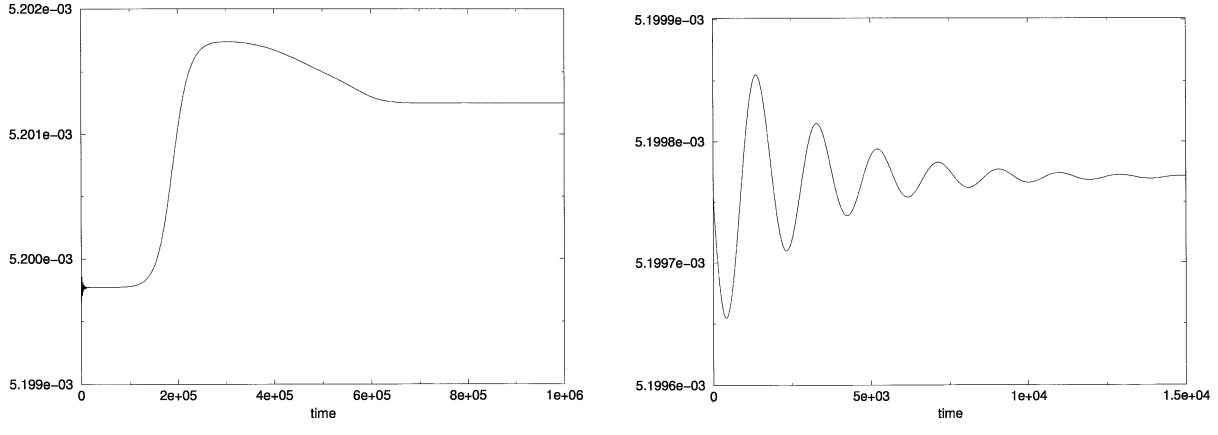

(a) (b)

Fig. 4. The integrated Fourier transform of the density profile of species X as function of the simulation time. The three time scales can be observed, (a) spiraling to the fixed point ($\lesssim 2 \times 10^4$ timesteps), (b) exponential growth of stable density modulations ($\lesssim 2 \times 10^5$ timesteps) and the diffusion of spots in order to form a regular pattern.

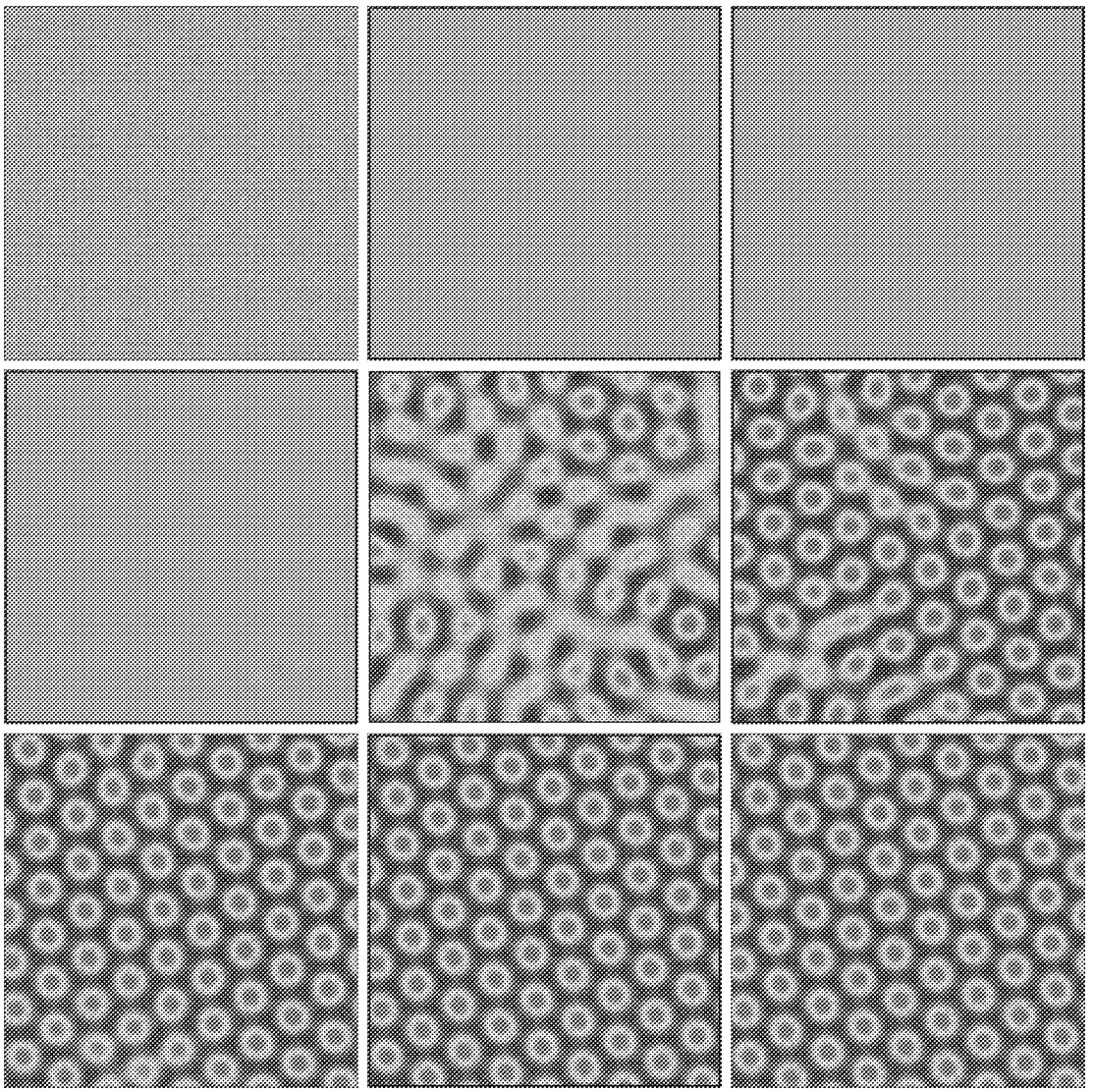

Fig. 5. Density profiles of species X in a 256×256 simulation on a square lattice. The snapshots are taken after, from left to right, 0, 2×10^4, 5×10^4, 10^5, 2×10^5, 4×10^5, 6×10^5, 8×10^5, and 10^6 timesteps.

the beginning of patterns. This creates gradients which enter the reaction equations and cause them to be no longer valid globally.

In the total simulation there are three time scales present, as can be seen in Fig. 4, where the integrated Fourier transform is plotted as a function of the simulation time. Initially there are oscillations, which correspond to the inwards spiral to the stable fixed point of the reaction equations, during which the initial random noise will diffuse and disappear and will take about 20–30 thousand time steps.

In the next stage the stable modes are probed from an almost homogeneous system, leading to a rapid grow and to the formation of a clear pattern (Fig. 5), which is reached after about 200 thousand time steps. The initial pattern which is formed for sufficiently

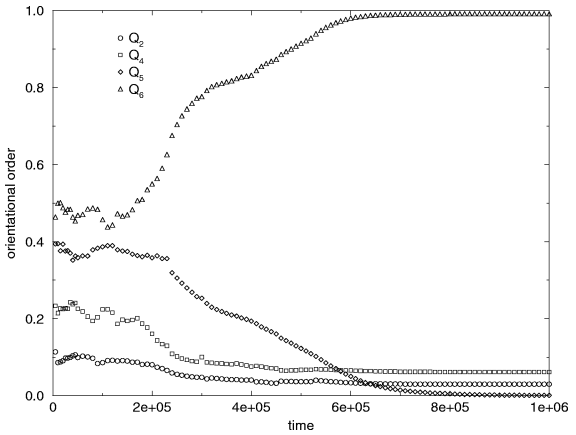

Fig. 6. Bond-orientational order of neighboring maxima of species X as function of time. Q_4 and Q_2 remain finite, indicating that no true six-fold symmetry is obtained.

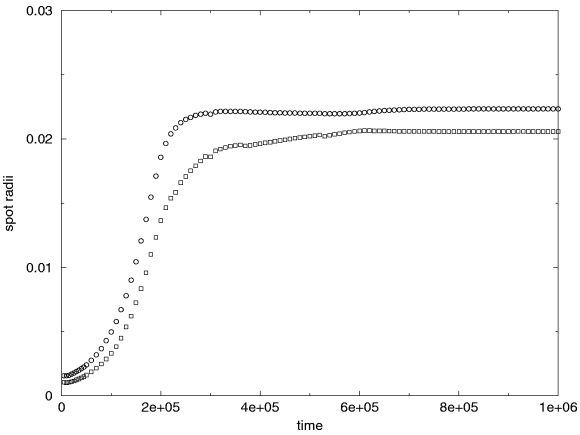

Fig. 7. The radii, describing the ellipsoidal shape of the maxima of species X, as function of time. The magnitude is a measure for the steepness of the maximum, the relative difference for the eccentricity. The circles and squares correspond to the average maximum and minimum radius, respectively.

large system, is formed a number of spots, with only some local order. In the last stage the spots start to rearrange themselves, forming a regular pattern, in a diffusion like process.

The characterization of the pattern and its evolution will depend on the underlying lattice of the simulation, because only a limited range of wave vectors are stable and can lead to pattern formation. From this continuous range, however, only few remain, i.e. those which will fit on the lattice used in the simulation. Their number is finite and depends on both the dimensions of the lattice and its symmetry.

In order to examine this we analyze the patterns in some more detail. As function of time we determine the locations of the extrema of the density profiles of both species. For species X we consider the maxima, while for species Y we take the minima, which are found at approximately the same locations in equilibrium. The shape of the spots is ellipsoidal, and in order to characterize them we fit the local density distribution within a distance of 5 lattice units by a second order polynomial. By doing so we find the value of the extremum, its off-lattice location, and the two radii of the ellipsoid. The outcomes are relatively insensitive to the size of the neighborhood if taken between 2 and 10 lattice units.

The number of spots shortly after the initialization is fairly high, and also the number of spots for species Y is larger. After about 5000 steps the number has decreased already to a value close to the final one. The relative difference between the magnitude of the extrema and the average density, however, is of the order 10^{-3} and 10^{-4} for species X and Y, respectively, and will continue to grow exponentially during the second time-scale of the process.

In order to analyze the local order of the spots we determine the location of neighboring spots using the Voronoi construction. This allows us to calculate the average distance between neighboring spots and bond-orientational order parameters

$$Q_l = \left\{ \langle \cos^2(l\phi) \rangle + \langle \sin^2(l\phi) \rangle \right\}^{1/2}, \tag{19}$$

where ϕ is the angle made by the line connecting two spots with the positive x-direction (Fig. 6).

As can be seen in the evolution of the pattern (Fig. 5), some spots merge after collision, while others split. As a consequence the average distance between spots is only a useful property near equilibrium, when this number remains fixed. The bond-orientational order parameters are less sensitive to the number of spots. Near equilibrium Q_6 goes to unity, as is necessary for a hexagonal pattern of spots. However, true six-fold symmetry is not obtained, because Q_4 and Q_2 do not go to zero, but remain finite, indicating that there is still a preferred direction.

This is also made clear by the two radii describing the ellipsoidal shape (Fig. 7). They differ about fifteen percent, indicating that a true six-fold symme-

try is not reached, because in that case it should be circular. These results are in agreement with the time evolution of a 256×296 system on a hexagonal lattice, which in real space has the same dimensions, and where relaxation parameters are chosen such that the theoretical diffusion coefficients in both simulations are identical. Although a complete comparison is not possible, due to the different random initialization in both cases, it does show that the overall behavior is similar, as it should. The distance between the extremes of the densities and bond-orientational order parameters agree within the accuracy of the computations.

This similarity is to be expected, since the macroscopic parameters describing the pattern are determined by the physical size of the system, which in both case is almost identical. If there is any influence of the lattice symmetry, it should be visible for small length scales. However, the height of the maximum density of species X is 1.374 and 1.372 on the square respectively hexagonal lattice, for species Y this is 0.265 and 0.270. The shape of the spots on the hexagonal lattice is slightly more ellipsoidal.

In conclusion, in the final equilibrium state only minor differences exist due to the lattice symmetry. The same is observed in other smaller system sizes. This does not mean that there is no influence of the lattice symmetry on the equilibrium situation, but that the size of the spots in units of lattice spacing is sufficiently large. It is obvious that on decreasing the size of the spots, the discrepancies between the two lattice symmetries become more visible. If for the present simulations a lattice symmetry dependence does exist, it could only be found in the evolution of the pattern formation. However, since the initial density distributions also influence this evolution, it is not possible to confirm or rule out the existence of a dependence of the underlying lattice.

6. Boundaries

The results shown in the previous section are all obtained in simulations using periodic boundary conditions. Periodic boundary conditions are of course a widely used trick in computer simulations to simulate small system sizes, and never the less retrieving information about much bigger systems. The trick however does not always give the desired result, as is the case here.

As we are interested in pattern formation, and want to obtain information about macroscopic systems, the periodic boundary conditions work here against us. There are two reasons, first of all the lattice size in combination with the lattice symmetry will only allow for certain length scales to be probed, i.e. those which fit nicely on a square lattice are (i, j), where $0 \leqslant i \leqslant M$ and $0 \leqslant j \leqslant M$ are arbitrary integers and M and N denote the lattice dimensions. The one with the largest positive growth rate in the infinite system, will in general not be among those, but can only be approximated.

There is, however, an additional problem coming from the periodic boundary conditions. As the Selkov model experiences a driving force to form a regular pattern, it encounters the boundary conditions, which impose constraints on the pattern. To clarify this, suppose that in an infinite system the optimal pattern would have stripes and the distance between two maxima would be 64. If the oscillation would be in the x-direction this would fit nicely on both a 64×32 and a 128×32 lattice. If the x-dimension of the lattice, however, would be anywhere in between 64 and 128, it does not fit exactly. Therefore, although the preferred length scale is present, due to the periodic boundary conditions, it can not be probed.

There are two types of boundaries we can impose which differ from the periodic ones. The one we will partially deal with here is walls, the other would be open boundaries. The former is important, since in most applications some impenetrable parts will be present, such as container walls or solid objects. The later could be used to avoid the coupling between the wave vectors and the lattice size.

The introduction of solid walls to the system, however, will have a different effect on the system. It will allow for all length scales present in the lattice, but the solid walls might act as a source of attractive force. In Fig. 8, the pattern evolution is shown for a 256×256 system on a square lattice, where we used bounce back on the links. The dynamical behavior in establishing a regular pattern is slower, as can be seen since the pattern is not yet stabilized after 10^6 time steps, while the one with periodic boundaries (Fig. 5),

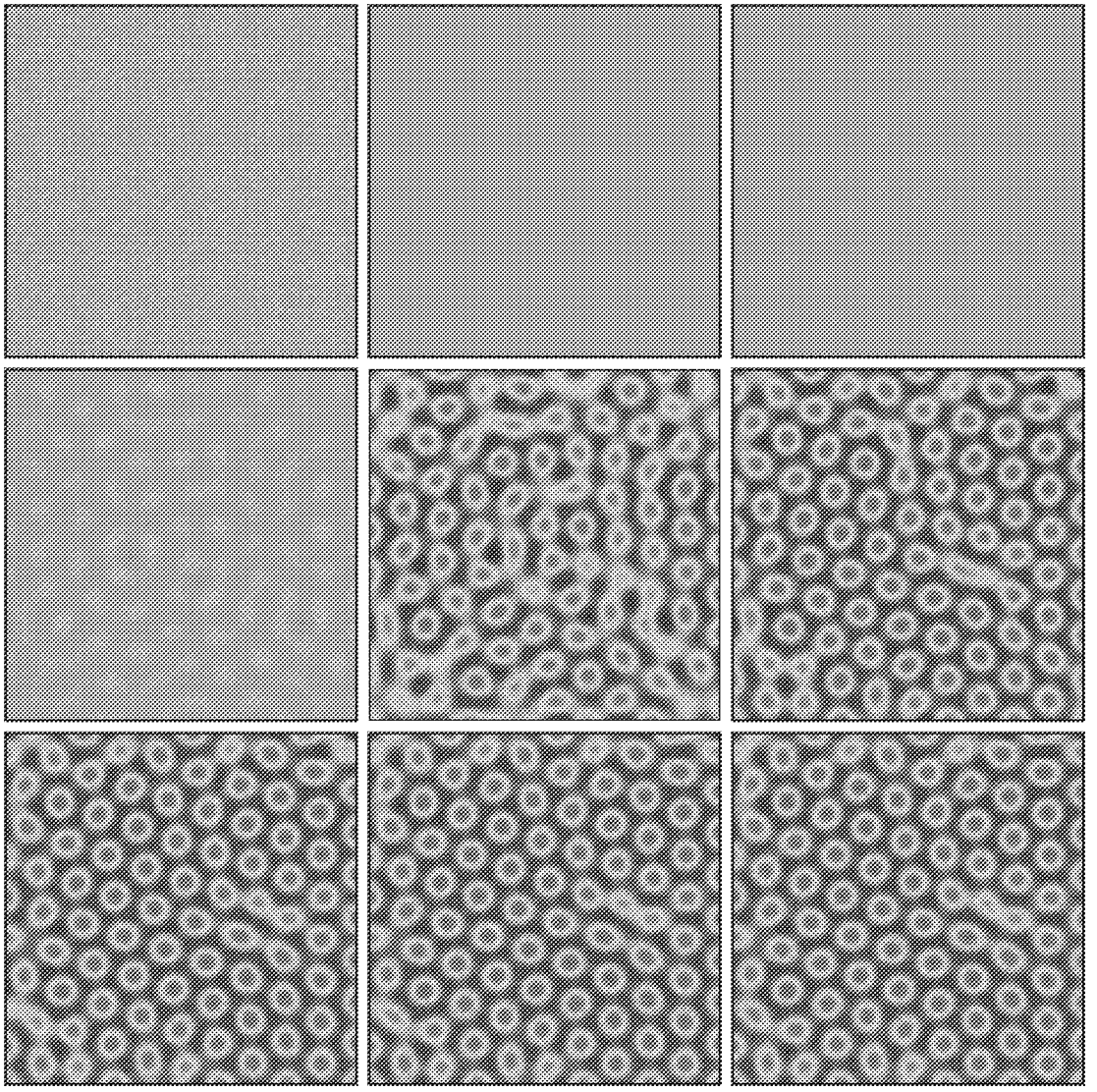

Fig. 8. Density profiles of species X in a 256×256 simulation on a square lattice with solid walls. The snapshots are taken after, from left to right, 0, 2×10^4, 5×10^4, 10^5, 2×10^5, 4×10^5, 6×10^5, 8×10^5, and 10^6 timesteps. Note the defect in the last four time-shots, which is not observed using periodic boundaries, that is slowly diffusing out of the system.

already is after 6×10^5. Moreover, the last three time-shots show a defect, that is slowly diffusing out of the system, while such a defect is not stable using periodic boundaries. Although there is no constrained to the length scales, the shape of the central spots, is on average still ellipsoidal and the walls seem to attract the spots.

7. Conclusion

We have performed reaction diffusion simulations in two dimensions. We used the Lattice Boltzmann method on various lattice sizes and two lattice symmetries, square and hexagonal. Depending on the application, care should be taken in the construction of

such a model, because size and symmetry of the lattice could influence the outcomes seriously.

By focusing on the influence of the underlying lattice on the formation of Turing patterns in the Selkov model, it is obvious that some finite size effects are encountered. The equilibrium results do not depend much on the symmetry of the lattice. If one is interested in a dynamical modeling of the system, this influence might still be present in the pattern evolution. However, in our simulations, where the dimension of the spot is of the order of 10 lattice units, no clear signature of the lattice symmetry is found.

One could of course adjust the simulation parameters in order to obtain smaller spot sizes, by decreasing the diffusion coefficients of both species. However, as a result the relaxation parameters would come too close to 0.5.

We indicated some preliminary results of simulations with boundary conditions other than periodic ones, namely solid walls. The evolution itself takes longer times to reach a truly equilibrium state. The removal of the periodic boundary conditions, releases the constraints on the patterns that can be formed. However, it also means that the "force" it exerts on the system to form a regular pattern is lost. Besides, also these boundaries influence the patterns, albeit in a different way.

References

[1] R. Kapral, A. Lawniczak, P. Masiar, Phys. Rev. Lett. 66 (1991) 2539.
[2] J. Dethier, F. Baras, M.M. Mansour, Europhys. Lett. 42 (1998) 19.
[3] Q. Ouyang, R. Li, G. Li, H.L. Swinney, J. Chem. Phys. 102 (1995) 2551.
[4] S. Ponce Dawson, S. Chen, G.D. Doolen, J. Chem. Phys. 98 (1993) 1514.
[5] D. Kandhai et al., Comput. Phys. Commun. 111 (1998) 14.
[6] A. Koponen et al., Phys. Rev. Lett. 80 (1998) 716.
[7] J.A. Kaandorp, C.P. Lowe, D. Frenkel, P.M.A. Sloot, Phys. Rev. Lett. 77 (1996) 2328.
[8] A.M. Turing, Philos. Trans. Roy. Soc. London, Ser. B 237 (1952) 37.
[9] E.E. Selkov, Eur. J. Biochem. 4 (1968) 79.
[10] J.D. Murray, Mathematical Biology, 2nd edn. (Springer, Berlin, 1993).